Practical quantum repeater using intense coherent light

Peter van Loock[1], Thaddeus D. Ladd[2], Kaoru Sanaka[2],
Fumiko Yamaguchi[2], Kae Nemoto[1], William J. Munro, Yoshihisa Yamamoto[1]
Trusted Systems Laboratory
HP Laboratories Bristol
HPL-2005-214
December 5, 2005*

quantum repeater, distributed entanglement, purification

We describe a practical quantum repeater protocol for long-distance quantum communication. In this scheme, entanglement is created between the intermediate nodes of the quantum channel by using a weak dispersive light-matter interaction and distributing the outgoing intense coherent light pulses among the nodes. Noisy entangled pairs of electronic spin are then prepared with high success probability via homodyne detection including postselection. The local gates for entanglement purification and swapping are deterministic and measurement-free, based upon the same coherent-light resources and weak interactions as for the initial entanglement distribution. Finally, the entanglement is stored in a nuclear-spin-based quantum memory. Simulations of the system show qubit-communication rates approaching 100Hz and fidelities above 99% for reasonable local gate errors.

* Internal Accession Date Only
[1]National Institute of Informatics, 2-1-2 Hitotsubashi, Chiyoda-ku, Tokyo 101-8430, Japan
[2]Edward L. Ginzton Laboratory, Stanford University, Stanford, CA 94305, USA
Approved for External Publication

Practical quantum repeater using intense coherent light

P. van Loock[1,*], T. D. Ladd[2,†], K. Sanaka[2,‡], F. Yamaguchi[2], Kae Nemoto[1], W. J. Munro[1,3], and Y. Yamamoto[1,2]

[1] *National Institute of Informatics, 2-1-2 Hitotsubashi, Chiyoda-ku, Tokyo 101-8430, Japan*

[2] *Edward L. Ginzton Laboratory, Stanford University, Stanford, California 94305, USA*

[3] *Hewlett-Packard Laboratories, Filton Road, Stoke Gifford, Bristol BS34 8QZ, United Kingdom*

We describe a practical quantum repeater protocol for long-distance quantum communication. In this scheme, entanglement is created between the intermediate nodes of the quantum channel by using a weak dispersive light-matter interaction and distributing the outgoing intense coherent light pulses among the nodes. Noisy entangled pairs of electronic spin are then prepared with high success probability via homodyne detection including postselection. The local gates for entanglement purification and swapping are deterministic and measurement-free, based upon the same coherent-light resources and weak interactions as for the initial entanglement distribution. Finally, the entanglement is stored in a nuclear-spin-based quantum memory. Simulations of the system show qubit-communication rates approaching 100 Hz and fidelities above 99% for reasonable local gate errors.

PACS numbers: 03.67.Hk, 42.25.Hz, 42.50.Dv

In a quantum repeater, long-distance entanglement is created by distributing entangled states over sufficiently short segments of a channel such that the noisy entangled states in each segment can be purified and then connected via entanglement swapping [1, 2]. The resulting entanglement between the distant nodes can then be used, for example, to teleport quantum information [3] or transmit secret classical information [4]. Existing approaches to quantum repeaters include a protocol based upon photon storage in atomic ensembles [5] and a scheme that uses solid-state photon emitters as the intermediate nodes of the channel [6, 7]. In these proposals, like in most proposals for quantum communication, *single photons* or very *weak coherent pulses* are being sent through the quantum channel. The single-photon schemes, however, naturally lead to very low communication rates.

More efficient schemes, compatible with existing classical optical communication networks, would involve multi-photon signals, i.e., light pulses of 10^4 or more photons. There are indeed various quantum communication protocols based on multi-photon Gaussian states [8]. However, entanglement purification, the essential step in a quantum repeater protocol, cannot be achieved within the realm of Gaussian states [9–11]. Similar to universal quantum computation [12], long-distance quantum communication requires a non-Gaussian element.

This non-Gaussian or nonlinear element may be introduced in at least two possible ways in order to achieve optical quantum computation. The first method uses only linear transformations, but a measurement-induced nonlinearity [13]. In the second approach, linear gates are supplemented by a weak nonlinear gate where the nonlinearity is effectively enhanced through a sufficiently strong probe beam [14]. Here we will apply the concept of weak nonlinearities to quantum communication via an optical electronic-spin and nuclear-spin hybrid system. For this purpose, we will be using *intense coherent pulses* of about 10^4 photons. A significant advantage of our proposal over the single-photon or weak coherent-state based protocols [6, 7] is that we can achieve high success probabilities via efficient homodyne detection of the intense coherent light pulses including postselection. Moreover, compared to the atomic-ensemble based schemes [5], we will avoid the complication of purifying an atomic ensemble and directly distill the entanglement from several copies of noisy entangled electronic-spin pairs. The electronic and nuclear spin systems may be achieved, for example, by single charged semiconductor quantum dots [15] or donors bound to semiconductor impurities [16] in high-Q microcavities.

In our proposal, every coherent "probe" pulse is subject to a reasonably weak nonlinear interaction with an electronic spin in a cavity. This interaction induces a conditional phase shift of the order of 10^{-2}, thus entangling the probe and the spin. After traveling over the communication channel, each probe will interact with a second spin. Noisy entangled pairs of distant electronic spins can then be prepared with success probability $P_{\text{success}} \approx 0.36$ via homodyne-detected postselection. The resulting initial fidelities $F_{\text{initial}} \approx 0.77$ may be increased by entanglement purification in advance to a nested entanglement swapping protocol with a number of qubits in each repeater station growing only logarithmically with communication distance [2]. For both purification and the Bell-state analysis required by the swapping procedure, we propose to use a deterministic measurement-free controlled-phase gate on the electronic spins based on the same conditional phase shifts with intense coherent light pulses [17]. This gate, though less tolerant to loss than the post-selected measurement-based gate used to generate initial entanglement, requires no postselection and may allow final end-to-end fidelities exceeding 0.99 with sufficiently small local optical losses. The entire quantum repeater protocol, including the entanglement distribution, entanglement purification, and deterministic entanglement swapping is all based on the same intense coherent-light resources and weak interactions. The resulting quantum repeater system is very tolerant to losses along the long-distance channel and can allow qubit-communication-rates of nearly 100 Hz over 1280 km with realistic optical fibers.

Figure 1 illustrates the mechanism for the entanglement distribution among the nearest nodes of the channel. The electron spin system is treated as a Λ-system, with two stable or metastable states $|g\rangle$ and $|e\rangle$, only one of which ($|e\rangle$) is resonant or nearly resonant with the cavity mode. Local rotations between states $|g\rangle$ and $|e\rangle$ may be achieved via stimulated Raman transitions or ESR pulses; in particular, we suppose the state is initially prepared in the state $(|g\rangle + |e\rangle)/\sqrt{2}$. The probe light is sufficiently detuned from the cavity to allow a strictly dispersive light-matter interaction. The finite probability for spontaneous emission of the qubit and for light to leak from the cavity add a small correction to channel losses, which we consider shortly. For clarity, let us first discuss entanglement distribution in the absence of loss. When the probe beam in coherent state $|\alpha\rangle$ reflects from the cavity, the total output state may be phenomenologically described by

$$\hat{U}_{\text{int}}\left[(|g\rangle + |e\rangle)\,|\alpha\rangle\right]/\sqrt{2} = \left(|g\rangle|\alpha\rangle + |e\rangle|\alpha e^{\imath\theta}\rangle\right)/\sqrt{2}\,, \quad (1)$$

where $\theta = \kappa t$ with κ equal to the coupling strength of the light-spin system and t the interaction time. After acquiring such a conditional phase shift at one node, the probe beam is sent to a neighboring node and interacts with a second spin in a similar way. Applying a further linear phase shift of $-\theta$ to the probe will yield the total state $(\sqrt{2}|\Psi^+\rangle|\alpha\rangle + |gg\rangle|\alpha e^{-i\theta}\rangle + |ee\rangle|\alpha e^{i\theta}\rangle)/2$, where $|\Psi^+\rangle = (|ge\rangle + |eg\rangle)/\sqrt{2}$. Thus, by discriminating a zero-phase shift from a $\pm\theta$ phase shift for the probe, one can project the two spins onto a maximally entangled state [14, 18]. Assuming α real, such a projection can be approached via a p quadrature measurement (i.e., along the imaginary axis in phase space), postselecting the desired $|\Psi^+\rangle$ state.

The conditional state of the spin system for a measured p value of the probe beam may now be written as

$$|\psi(p)\rangle = \frac{1}{2}\left[\sqrt{2}\,G_0(p)\,|\Psi^+\rangle + G_-(p)\,|gg\rangle + G_+(p)\,|ee\rangle\right], \quad (2)$$

where $G_0(p) \equiv f_0(p)g_0(p)$ is a Gaussian amplitude function with $f_0(p) = (2/\pi)^{1/4}\exp(-p^2)$ and a phase factor $g_0(p) = \exp(-2i\alpha p)$, depending on the measurement result. Similarly, we have $G_\pm(p) \equiv f_\pm(p)g_\pm(p)$ with the displaced Gaussians $f_\pm(p) = (2/\pi)^{1/4}\exp[-(p \mp d)^2]$ and $g_\pm(p) = \exp[-i\alpha\cos\theta(2p \mp d)]$. Here, our ability to distinguish the desired $|\Psi^+\rangle$ state (around zero phase shift of the probe) and the two unwanted terms corresponding to the two phase-rotated probe beams shifted along the p axis by $\pm d$ is determined by the distance of the corresponding Gaussian peaks, $d = \alpha\sin\theta$. In the following, this parameter d is referred to as the *distinguishability*. The maximally entangled state is postselected by keeping the state only when the measured result p is within some finite measurement window, $|p| < p_c$. Were it not for optical losses, a very large window could be chosen, because by increasing α, the distinguishability could be made even larger, resulting in nearly perfect post-selection with probability of success 1/2. However, in the presence of loss, there will be a trade-off between distinguishability and decoherence. Let us now consider this realistic case including losses.

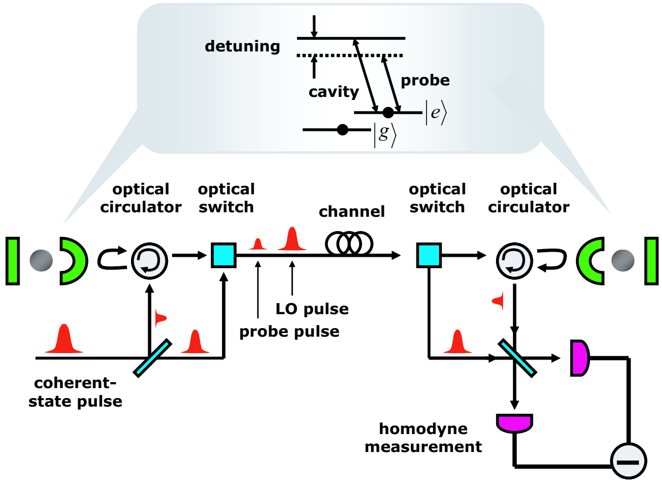

FIG. 1: (Color online). Schematic for the generation of spin-entanglement between two qubits at neighboring stations via homodyne detection discriminating between conditionally phase-rotated coherent probe beams.

In the presence of channel loss (and a small contribution from cavity losses and spontaneous emission), the distinguishability cannot be made arbitrarily large without suffering from intolerable decoherence. We may model the photon loss by considering a beam splitter in the channel that transmits only a part of the probe beam with an intensity transmission η^2. The lost photons split from the channel by this beam splitter provide "which-path" information, and tracing over them introduces the decoherence. After the homodyne detection of the probe, the spins are described by an unnormalized conditional density matrix $\hat{\rho}(p)$ which depends on the measurement result p and has the following diagonal elements:

$$\begin{aligned} \rho_{\Psi^\pm,\Psi^\pm} &= |G_0(p)|^2 \mathrm{Re}\lambda_\pm(\xi)/2, \\ \rho_{\Phi^\pm,\Phi^\pm} &= (|G_-(p)|^2 + |G_+(p)|^2)/8 \\ &\quad \pm e^{-\gamma}\mathrm{Re}[e^{i\xi}\mathcal{G}_{+-}(p)], \end{aligned} \quad (3)$$

written in the Bell basis $\{|\Psi^\pm\rangle, |\Phi^\pm\rangle\}$, with $|\Psi^\pm\rangle = (|ge\rangle \pm |eg\rangle)/\sqrt{2}$ and $|\Phi^\pm\rangle = (|gg\rangle \pm |ee\rangle)/\sqrt{2}$, and using $\lambda_\pm(\xi) \equiv (1 \pm e^{-\gamma + i\xi})/2$ and $\mathcal{G}_{+-}(p) \equiv G_+(p)G_-^*(p)/4$, etc. In the functions $g_0(p)$ and $g_\pm(p)$, α is replaced by $\eta\alpha$, and the distinguishability now becomes $d = \eta\alpha \sin\theta \approx \eta\alpha\theta$. The decoherence in the channel leads to a damping factor determined by

$$\gamma = \alpha^2(1-\eta^2)(1-\cos\theta) \approx \frac{1}{2}(1-\eta^2)d^2/\eta^2 \,, \tag{4}$$

and an additional phase factor with $\xi \equiv \alpha^2(1-\eta^2)\sin\theta$. The off-diagonal elements are given by

$$\begin{aligned}
\rho_{\Psi^\pm,\Psi^\mp} &= i|G_0(p)|^2 \mathrm{Im}\lambda_\pm(\xi)/2, \\
\rho_{\Phi^\pm,\Phi^\mp} &= (|G_-(p)|^2 - |G_+(p)|^2)/8 \\
&\quad \pm ie^{-\gamma}\mathrm{Im}[e^{i\xi}\mathcal{G}_{+-}(p)], \\
\rho_{\Psi^\pm,\Phi^\pm} &= \rho^*_{\Phi^\pm,\Psi^\pm} = \mathcal{G}_{0-}(p)\lambda_\pm(\xi) + \mathcal{G}_{0+}(p)\lambda_\pm(-\xi), \\
\rho_{\Psi^\pm,\Phi^\mp} &= \rho^*_{\Phi^\mp,\Psi^\pm} = \mathcal{G}_{0-}(p)\lambda_\pm(\xi) - \mathcal{G}_{0+}(p)\lambda_\pm(-\xi).
\end{aligned} \tag{5}$$

Here we see that in order to maximize the distinguishability of the probe states (and hence the fidelity of the resulting entangled state), we cannot simply make d arbitrarily large. An arbitrarily large d value would be accompanied by an arbitrary increase of the decoherence effect. This is reflected by the d-dependence of the loss parameter γ and may, at worst, lead to a separable output state $\hat{\rho}(p)$. The parameter ξ determines a fixed (measurement result-independent) and known phase rotation which can be easily removed via static phase shifters. Thus, in the above matrix elements, we set $\xi \equiv 0$.

Since we cannot make d arbitrarily large, we are forced to choose a sufficiently small window for the postselection, thus making p_c sufficiently small. This will lead to a decreasing success probability. As a result, there will also be a trade-off between the success probability after postselection and the fidelity of the outgoing entangled states [19]. The success probability can be calculated as

$$\begin{aligned}
P_{\mathrm{success}} &= \mathrm{Tr}\int_{-p_c}^{+p_c} dp\,\hat{\rho}(p) = \int_{-p_c}^{+p_c} dp\,\mathrm{Tr}\hat{\rho}(p) \\
&= \frac{1}{4}\left[2\,\mathrm{erf}(\sqrt{2}p_c) + \mathrm{erf}(b_+) + \mathrm{erf}(b_-)\right],
\end{aligned} \tag{6}$$

where $\mathrm{Tr}\hat{\rho}(p)$ is the "single-shot" probability for obtaining the quadrature value p with the diagonal elements of $\hat{\rho}(p)$ from Eq. (3). Here, we used $b_\pm \equiv \sqrt{2}(p_c \pm d)$. The desired entangled output state is $|\Psi^+\rangle$. Hence, the average fidelity after postselection becomes [20]

$$\begin{aligned}
F &= \left[\int_{-p_c}^{+p_c} dp\,\langle\Psi^+|\hat{\rho}(p)|\Psi^+\rangle\right] \Big/ P_{\mathrm{success}} \\
&= \frac{\mathrm{erf}(\sqrt{2}p_c)(1+e^{-\gamma})}{2\,\mathrm{erf}(\sqrt{2}p_c) + \mathrm{erf}(b_+) + \mathrm{erf}(b_-)},
\end{aligned} \tag{7}$$

using Eq. (3).

We assume that loss is dominated by fiber loss in the quantum channel. A practical length for the individual segments of the quantum repeater system would be $l_0 = 10$ km. Assuming a transmission loss of about

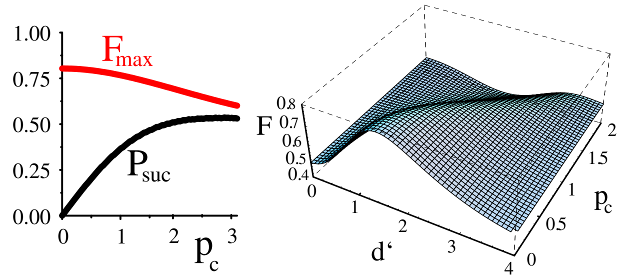

FIG. 2: (Color online). On the right: the fidelity of the outgoing entangled state as a function of the distinguishability parameter $d' \equiv \alpha\theta$ and the size of the postselection window p_c. On the left: the maximum fidelity F_{max} and success probability P_{suc} as a function of the postselection window p_c. For all plots, $\eta^2 = 2/3$.

0.17 dB/km, the transmission parameter η^2 is about 2/3. In Fig. 2, the average fidelity is shown as a function of $d' \equiv \alpha\theta$ and p_c for a transmission of $\eta^2 = 2/3$. The plot illustrates the trade-off between distinguishability and decoherence, leading to an optimal value for d' for each p_c. However, the maximum average fidelity of $F \approx 0.8$ can be achieved only at the expense of a vanishing success probability. Now by choosing a slightly larger postselection window and sacrificing a little bit of the fidelity, $F \approx 0.77$, we can attain a reasonable success probability, $P_{\mathrm{success}} \approx 36\%$. This high rate of successful entanglement generation is in sharp contrast to the low efficiencies of single-photon or weak-coherent-state approaches [6, 7].

Our initial fidelities, $F_{\mathrm{initial}} \approx 0.77$, will be insufficient for entanglement swapping; some entanglement purification must first occur. For both purification and swapping, local two-qubit gates are needed. For this purpose, we propose to use measurement-free deterministic controlled-phase gates [17]. The advantage of such gates is that they can be implemented using the same intense coherent-light resources and weak interactions as employed in the above entanglement distribution protocol. The controlled-phase gate can be realized via the following sequence of conditional rotations and unconditional displacements of a coherent-state probe interacting with the two spins [17],

$$\hat{U}_2(\theta)\hat{D}(\beta)\hat{U}_1(\theta)\hat{D}(-\beta^*)\hat{U}_2(\theta)\hat{D}(-\beta)\hat{U}_1(\theta)\,, \tag{8}$$

where $\hat{U}_k(\theta)$ corresponds to the interaction in Eq. (1), leading to a controlled phase shift of the probe conditioned upon the state of the kth qubit. The operator $\hat{D}(\beta)$ describes a phase-space displacement of the probe where $\beta \equiv \alpha(1-i)$. After the entire sequence in Eq. (8), the probe will be nearly disentangled from the spins. After tracing over the probe and removing single-qubit Z-rotations, the qubits have undergone a controlled rotation of angle $\phi \approx \alpha^2\theta^2(6T_1T_2T_3 - T_1T_2 - T_1)$, where T_j is the transmission for the jth cavity-probe interaction. For a desired phase shift of the order of π, we must satisfy

$\alpha^2\theta^2 \approx 1$, which is exactly the regime we have been using for the entanglement distribution. A small amount of decoherence is also introduced due to the finite probe-qubit entanglement and any finite optical loss. The details of this decoherence mechanism will be discussed elsewhere [21]. Two-qubit coherences are damped by factors similar to $\exp(-\theta^2+\epsilon)$, where $\epsilon = 1 - T_j$. For optical losses between $\epsilon = 0.01\%$ and $\epsilon = 0.1\%$, errors caused by this gate saturate due to the finite probe-qubit entanglement; in a practical implementation, the gate's performance will likely be limited by optical losses rather than the θ^2 term.

This controlled-sign gate, in addition to single-qubit rotations and measurement (which may also be done by homodyne detection of an intense optical probe, or by other methods) are sufficient resources for the standard purification protocol introduced in Ref. 22. This protocol was analyzed in terms of density matrices $\hat{\rho}$ that are exactly diagonal in the Bell-state basis. The $\hat{\rho}$ described in Eqs. (3-5) is very nearly so, and the small off-diagonal elements quickly vanish after a few purification steps. It was previously noted [2] that this protocol converges faster than protocols based on Werner states [23].

Several protocols for combining entanglement purification and swapping to connect large distances have been previously considered. At one extreme in the number of qubit resources is "scheme B" of Dür et al. [2]. This scheme uses as many qubits as are needed to allow rapid parallel purification; for communication over 1000 km, hundreds of qubits are needed in each repeater station. At the other extreme is the scheme of Childress et al. [6, 7] in which only two qubits are needed in each repeater station, but the process of purification and swapping is very slow and becomes impossible if the initial pair-fidelities are too low and if gate errors are too high.

We consider a protocol in between these two extremes; we find that with a number of qubits per station which grows only logarithmically with distance, a reasonable communication qubit-rate with reasonable gate errors may be achieved. In this scheme, each repeater station acts autonomously according to a simple set of rules. After responding to communications received from other repeater stations, each station attempts to swap qubits so as to double the distance over which pairs are entangled. If no qubits are available for swapping, each attempts to purify pairs entangled over the same distance at the highest fidelities available. Then, any qubits not entangled are immediately entangled with available qubits in nearest-neighbor nodes. The minimum number of qubits required at the endpoint and middle repeater stations for this scheme to complete is $N = 2 + 2\log_2(L/l_0)$, where L is the total length of the channel and l_0 is the distance between stations. For example, for communication over 1280 km with repeater stations separated by 10 km, this scheme requires 16 qubits per station (with 8 parallel quantum channels connecting each ad-

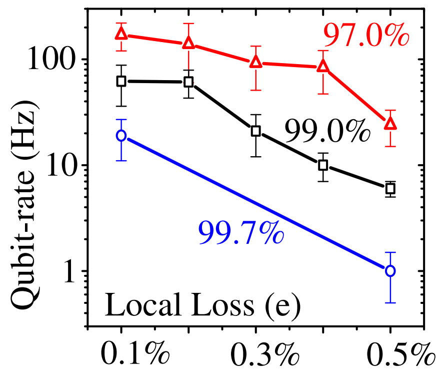

FIG. 3: (Color online). Achievable qubit communication results (in terms of qubit rates for different target fidelities) vs. local optical losses (ϵ). Each point corresponds to a single Monte-Carlo simulation of the nested purification protocol over 9 complete qubit teleportations; each point is the average difference in time between teleported qubit arrival times, and the error bar is the standard deviation.

jacent station) with fast optical switches to allow any channel to interact coherent probes with any qubit in each station. This scheme is similar to "scheme C" of Dür et al. [2], except by putting N qubits at *every* station the probabilistic generation of initial pairs and the purification of short-distance entanglement proceeds more quickly. Since every long-distance purification step requires a foundation of short-distance entanglement generation, speeding these initial steps can lead to substantial speed-up for only a small number of added qubits.

The quantum communication rate achieved by this scheme is calculated via Monte-Carlo simulation with numbers of purification steps at each distance chosen by threshold criteria designed to obtain final long-distance fidelities in the vicinity of 99%. In these simulations it is assumed that the limiting timescale is the time for light to propagate over the 10 km distance between repeaters, about 50 μs. Larger fidelities are possible at smaller rates, and larger rates are available at smaller final fidelities. Of course, the rates and fidelities drop due to local gate error; for our calculations we presume that error is dominated by optical loss. Fig. 3 shows typical rates for different target fidelities and different amounts of local optical loss. Further discussion of the scaling behavior will appear elsewhere [21].

Two more technical issues should be raised. First, the time for optical information to propagate over 1280 km in optical fibers, about 6 ms, is already longer than decoherence times observed in most solid-state electronic spin systems; to this one must consider the additional time required to await the entanglement purification and swapping. While quantum error correction techniques may in principle be employed to extend spin coherence times, the introduction of nuclear memory is likely a sufficient and less expensive resource, as decoherence timescales for isolated nuclei should be at least many seconds [24] and probably longer. For isolated nuclei, fast ENDOR (electron-nuclear double resonance) pulse techniques may be employed for rapid storage and retrieval of the electron-spin state [25]. Nuclear ensembles in quantum dots have also been considered [26], but in this case the decoupling-limited memory time is likely to be shorter. The second technical consideration is that the loss-rates we have assumed over the long-distance communication channel have assumed telecom wavelengths, while the solid-state emitter is likely to operate at shorter wavelengths, so efficient phase-preserving wavelength conversion of the strong optical probe is required.

In summary, we proposed a full quantum repeater system based upon weak dispersive light-matter interactions between small numbers of solid-state electronic spin qubits in microcavities and intense coherent light pulses. Using a nested purification protocol, qubit-rates up to 100 Hz and final fidelities of 99% are possible. The practicality and efficiency of this proposal results from its high success probabilities for the initial entanglement distribution (around 40%) and its tolerance to loss in the long-distance channel.

The authors thank Lily Childress for useful discussions.

---

* Electronic address: vanloock@nii.ac.jp

† Electronic address: tladd@stanford.edu; also at Institute of Industrial Science, University of Tokyo, Japan.

‡ Also at Institute of Industrial Science, University of Tokyo, Japan.

[1] H.-J. Briegel, W. Dür, J. I. Cirac and P. Zoller, Phys. Rev. Lett. **81**, 5932 (1998).

[2] W. Dür, H.-J. Briegel, J. I. Cirac and P. Zoller, Phys. Rev. A **59**, 169 (1999).

[3] C. H. Bennett *et al.*, Phys. Rev. Lett. **70**, 1895 (1993).

[4] A. K. Ekert, Phys. Rev. Lett. **67**, 661 (1991).

[5] L. M. Duan, M. D. Lukin, J. I. Cirac, and P. Zoller, Nature **414**, 413 (2001).

[6] L. Childress, J. M. Taylor, A. S. Sørensen, and M. D. Lukin, eprint: quant-ph/0410123 (2005).

[7] L. Childress, J. M. Taylor, A. S. Sørensen, and M. D. Lukin, eprint: quant-ph/0502112 (2005).

[8] S. L. Braunstein and P. van Loock, Rev. Mod. Phys. **77**, 513 (2005).

[9] J. Eisert, S. Scheel and M. B. Plenio, Phys. Rev. Lett. **89**, 137903 (2002).

[10] J. Fiurášek, Phys. Rev. Lett. **89**, 137904 (2002).

[11] G. Giedke and J. I. Cirac, Phys. Rev. A **66**, 032316 (2002).

[12] S. Lloyd and S. L. Braunstein, Phys. Rev. Lett. **82**, 1784 (1999).

[13] E. Knill, R. Laflamme, and G. J. Milburn, Nature **409**, 46 (2001).

[14] K. Nemoto and W. J. Munro, Phys. Rev. Lett. **93**, 250502 (2004).

[15] D. Englund *et al.*, Phys. Rev. Lett. **95**, 013904 (2005); A. S. Bracker *et al.*, Phys. Rev. Lett. **94**, 047402 (2005).

[16] S. Strauf *et al.*, Phys. Rev. Lett. **89**, 177403 (2002); K-M. C. Fu, T. D. Ladd, C. Santori, and Y. Yamamoto, Phys. Rev. B **69**, 125306 (2004).

[17] T. P. Spiller *et al.*, eprint: quant-ph/0509202 (2005).

[18] W. J. Munro, K. Nemoto, and T. P. Spiller, New Journal of Physics **7**, 137 (2005).

[19] One could imagine increasing the success probability by choosing a measurement scheme that also postselects the $|\Phi^+\rangle$ state. Neglecting losses, this is possible using x-homodyne detection (along the real axis in phase space) rather than p-homodyne detection [18]. However, in this case the distinguishability scales as $\alpha\theta^2$, which in order to be kept of order unity requires extremely intense pulses with α scaling as θ^{-2}. The loss parameter γ then also scales as θ^{-2}, leaving almost no coherence at all in the final entangled state. In another possible detection scheme, with similar scaling to the p measurement, one may shift the coherent states back to the phase-space origin and discriminate between zero and non-zero photons [18].

[20] Here we assume no information is used by each repeater station as to which p value within the measurement window was obtained. A further optimized system could change its behavior depending on the measured value of p for improved performance.

[21] T. D. Ladd *et al.*, in preparation.

[22] D. Deutsch, A. Ekert, R. Jozsa, C. Macchiavello, S. Popescu, and A. Sanpera, Phys. Rev. Lett. **77**, 2818 (1996).

[23] C. H. Bennett, G. Brassard, S. Popescu, B. Schumacher, J. A. Smolin, and W. K. Wootters, Phys. Rev. Lett. **76**, 722 (1996).

[24] T. D. Ladd *et al.*, Phys. Rev. B **71**, 014401 (2005).

[25] F. Jelezko *et al.*, Phys. Rev. Lett. **93**, 130501 (2004).

[26] J. M. Taylor, C. M. Marcus, and M. D. Lukin, Phys. Rev. Lett **90**, 206803 (2003).